A General Approach for Detecting Folding Intermediates from Steady-State and Time-Resolved Fluorescence of Single-Tryptophan-Containing Proteins
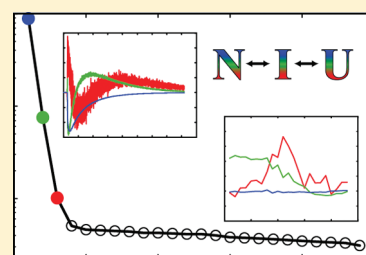
Sergey P. Laptenok,[†,‡,||] Nina V. Visser,[‡] Ruchira Engel,[§,⊥] Adrie H. Westphal,[§] Arie van Hoek,[‡] Carlo P. M. van Mierlo,[§] Ivo H. M. van Stokkum,[†] Herbert van Amerongen,*[,‡] and Antonie J. W. G. Visser[§]

[†]Department of Physics and Astronomy, Faculty of Exact Sciences, Vrije Universiteit Amsterdam, De Boelelaan 1081, 1081 HV Amsterdam, The Netherlands

[‡]Laboratory of Biophysics and [§]Laboratory of Biochemistry, Microspectroscopy Centre, Wageningen University, P.O. Box 8128, 6700 ET Wageningen, The Netherlands

S *Supporting Information*

ABSTRACT: During denaturant-induced equilibrium (un)folding of wild-type apoflavodoxin from *Azotobacter vinelandii*, a molten globule-like folding intermediate is formed. This wild-type protein contains three tryptophans. In this study, we use a general approach to analyze time-resolved fluorescence and steady-state fluorescence data that are obtained upon denaturant-induced unfolding of a single-tryptophan-containing variant of apoflavodoxin [i.e., W74/F128/F167 (WFF) apoflavodoxin]. The experimental data are assembled in matrices, and subsequent singular-value decomposition of these matrices (i.e., based on either steady-state or time-resolved fluorescence data) shows the presence of three significant, and independent, components. Consequently, to further analyze the denaturation trajectories, we use a three-state protein folding model in which a folding intermediate and native and unfolded protein molecules take part. Using a global analysis procedure, we determine the relative concentrations of the species involved and show that the stability of WFF apoflavodoxin against global unfolding is ∼4.1 kcal/mol. Analysis of time-resolved anisotropy data of WFF apoflavodoxin unfolding reveals the remarkable observation that W74 is equally well fixed within both the native protein and the molten globule-like folding intermediate. Slight differences between the direct environments of W74 in the folding intermediate and native protein cause different rotameric populations of the indole in both folding species as fluorescence lifetime analysis reveals. Importantly, thermodynamic analyses of the spectral denaturation trajectories of the double-tryptophan-containing protein variants WWF apoflavodoxin and WFW apoflavodoxin show that these variants are significantly more stable (5.9 kcal/mol and 6.8 kcal/mol, respectively) than WFF apoflavodoxin (4.1 kcal/mol) Hence, tryptophan residues contribute considerably to the 10.5 kcal/mol thermodynamic stability of native wild-type apoflavodoxin.

Because of their sensitivity and multiparameter capacity, fluorescence techniques are widely utilized to obtain thermodynamic and kinetic information about protein folding (for a review, see ref 1). The fluorescent probe employed most frequently in folding studies is tryptophan, because the fluorescence parameters of the indole chromophore (i.e., spectrum, quantum yield, and lifetime) are highly sensitive to changes in the local environment and because many proteins contain this amino acid residue. Thermodynamic parameters that characterize a two-state unfolding transition, in which native and unfolded states interconvert, can be easily derived from analysis of steady-state fluorescence spectra and fluorescence decay kinetics of single-tryptophan-containing proteins, as shown, for example, for nuclease A from *Staphylococcus aureus*.[1] When one or more intermediate folding states are populated during equilibrium (un)folding of a protein, more complex thermodynamic models need to be taken into account.[1]

In this study, we use a single-tryptophan mutant of the 179-residue apoflavodoxin (i.e., flavodoxin without cofactor FMN)

from *Azotobacter vinelandii* to allow analysis of steady-state and time-resolved fluorescence data that are obtained upon denaturant-induced unfolding of this protein. Guanidine hydrochloride (GuHCl) is employed as a denaturant. Wild-type apoflavodoxin is a prototype for the investigation of denaturant-induced protein (un)folding and forms a molten globule-like intermediate during its equilibrium (un)folding (see refs 2–6).

The three-dimensional structure of native wild-type flavodoxin from *A. vinelandii* is characterized by a five-stranded parallel β-sheet that is surrounded by α-helices.[7] This α–β parallel topology is a commonly observed fold. Native apoflavodoxin is structurally identical to flavodoxin except for dynamic disorder in the flavin-binding region.[8] The fluorescence of native apoflavodoxin arises mainly from its three tryptophans (i.e., W74, W128,

and W167). W74 is located in α-helix 3; W128 is close to β-strand 5a, and W167 is in α-helix 5 of the protein. Using time-resolved fluorescence anisotropy, we recently demonstrated that photoexcited tryptophan residues of wild-type apoflavodoxin exchange energy through a Förster type of dipolar coupling mechanism.[4,9] The transfer of energy from W167 to W128, residues that are 6.8 Å apart, has been revealed by this methodology, because this transfer leads to rapid decay of the anisotropy signal with a 50 ps transfer correlation time. To avoid the type of complications that are associated with the analysis of time-resolved fluorescence (un)folding data of multi-tryptophan-containing proteins, we use in this study the single-tryptophan variant W74/F128/F167 (WFF) of apoflavodoxin. In this variant, both W128 and W167 are substituted with phenylalanine residues, thus leaving W74 as the single fluorescent probe.

We monitor the GuHCl-induced unfolding of WFF apoflavodoxin through acquisition of steady-state fluorescence spectra and time-resolved fluorescence data. The resulting family of unfolding curves obtained in a particular fluorescence experiment is called a denaturation trajectory. The experimental data are assembled in a matrix, and subsequent singular-value decomposition (SVD)[10,11] of this matrix allows determination of the number of different species that are formed during the equilibrium unfolding of the protein. Although there are many applications of SVD, it is used here to estimate the rank of the data matrix to identify the number of dimensions along which the experimental data that exhibit the largest variations. In both matrices obtained (i.e., based on either steady-state or time-resolved fluorescence data), SVD shows the presence of three significant, and independent, components. Consequently, to further analyze the data, we use a three-state protein folding model in which a folding intermediate and native and unfolded protein molecules take part.[2–6] Each set of experimental data is globally analyzed using this model, which yields relative concentrations of all species along the denaturation trajectory and thereby reveals their thermodynamic properties.

We also employ fluorescence anisotropy decay to probe denaturant-induced equilibrium unfolding of WFF apoflavodoxin. As outlined in ref 1, in this type of measurement extraction of the thermodynamic properties of the folding species involved is not straightforward, because anisotropy does not keep direct track of the population of folding states involved. Instead, the time-dependent anisotropy of the species involved needs to be weighted by their fluorescence intensity components. In addition, anisotropy decays of unfolded protein conformations exhibit correlation times characteristic of rapid segmental motions, which are superimposed on correlation times arising from slow overall protein tumbling. For this reason, the unfolding trajectory of WFF apoflavodoxin as measured by fluorescence anisotropy has first been analyzed using a single- or double-exponential decay model for each individual anisotropy decay trace. Subsequently, a global analysis strategy is applied to retrieve the relative populations of the different states involved during unfolding of the protein.

Finally, to assess the effects that deletion of tryptophan residues has on native apoflavodoxin stability, we use two apoflavodoxin variants in which two wild-type tryptophans are present [i.e., W74/W128/F167 (WWF) and W74/F128/W167 (WFW) apoflavodoxin] and follow their denaturant-induced equilibrium unfolding by acquiring steady-state fluorescence spectra. In both protein variants, either W128 or W167 is replaced with phenylalanine. The resulting data are subjected to the same thermodynamic analysis described above.

■ EXPERIMENTAL PROCEDURES

Materials, Protein Expression, and Protein Purification. All chemicals used were of the highest purity available. The concentration GuHCl was determined by measuring the refractive index of the sample used, as described previously.[4] Variants of flavodoxin, which contain either a single tryptophan (i.e., WFF flavodoxin) or two tryptophan residues [i.e., W74/W128/F167 (WWF) and W74/F128/W167 (WFW) flavodoxin], were obtained and purified as described previously.[4] We subsequently prepared apoflavodoxin by trichloroacetic acid precipitation, washing the FMN-free precipitate, and redissolving the apoprotein in buffer. In all experiments, the protein concentration was 4 μM in 100 mM potassium pyrophosphate buffer (pH 6.0). The temperature during all fluorescence experiments was set to 25 °C.

Steady-State Fluorescence Spectra and Time-Resolved Fluorescence Experiments. Steady-state fluorescence spectra were recorded with a Fluorolog 3.2.2 spectrofluorometer (Horiba, Jobin Yvon, Optilas, Alphen aan den Rijn, The Netherlands), as described previously.[4] The excitation wavelength was 300 nm; excitation and emission slit widths were 2 nm, and emission spectra were recorded between 310 and 400 nm with 1 nm steps. All spectra were corrected for wavelength-dependent instrumental response characteristics. Background fluorescence emission was measured under the same circumstances, except that now no protein is present in the samples, and was subsequently subtracted from the corresponding fluorescence spectra of samples with protein.

Time-resolved fluorescence measurements were performed using the time-correlated single-photon counting technique, as described previously.[4] Laser excitation was at 300 nm, and the duration of the pulse was less than 0.2 ps; pulse energies were at the picojoule level, and the repetition rate of excitation pulses was 3.8×10^6 pulses/s. The sample volume was 1 mL in 10 mm light-path fused silica cuvettes. The emission filter was a Schott UV DIL interference filter (Schott, Mainz, Germany), transmitting at 348.8 nm with a bandwidth of 5.4 nm. Fluorescence decay curves were collected in 4087 channels of a multichannel analyzer with a 5 ps spacing time per channel. Measurements consisted of 10 repeated cycles with a duration of 10 s of parallel $[I_\parallel(t)]$ and perpendicular $[I_\perp(t)]$ polarized fluorescence emission. Background emission was measured under the same conditions and subtracted from the individual decay traces of the sample involved. For the purpose of deconvolution, the dynamic instrumental response function was determined using freshly prepared solutions of p-terphenyl in a 50/50 (v/v) mixture of cyclohexane and CCl_4, which have a fluorescence lifetime of 14 ps.[4]

The total fluorescence decay $[I(t) = I_\parallel(t) + 2I_\perp(t)]$ was analyzed using a sum of discrete exponentials with lifetimes τ_i and amplitudes α_i, as described in ref 4. The fluorescence anisotropy decay $\{r(t) = [I_\parallel(t) - I_\perp(t)]/I(t)\}$ was also analyzed as described in ref 4. All anisotropy decay curves were first analyzed individually. The minimum model employed to analyze the anisotropy data consists of a single exponential with correlation time ϕ_2 and amplitude β_2. When the anisotropy turns out to decay with an additional, rapidly decaying component, another exponential term (with correlation time ϕ_1 and amplitude β_1) was included in the model to fit the data. The confidence limits of the correlation times at the 67% confidence level were determined using the exhaustive search approach.[12,13]

Singular-Value Decomposition. Two types of experiments were performed on apoflavodoxin in increasing concentrations of guanidine hydrochloride (GuHCl), namely, time-resolved fluorescence and steady-state fluorescence. The time-resolved
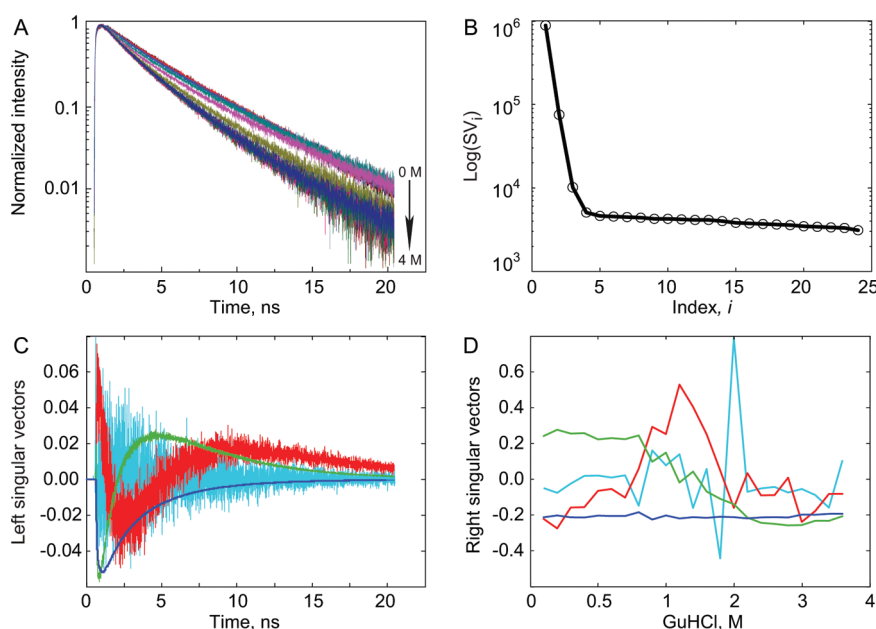
Figure 1. Analysis of time-resolved fluorescence data obtained from denaturant-induced unfolding of WFF apoflavodoxin. (A) Denaturation trajectory of time-resolved fluorescence data obtained at increasing concentrations of denaturant. Traces are normalized to their maximum fluorescence values and are subsequently aligned to the time point at which half of the rising part of fluorescence is reached. (B) Singular-value decomposition of the corresponding data matrix shows the presence of three significant components (singular vectors, SVs). (C) These SVs (colored dark blue, green, and red) show structure, while the fourth SV (light blue) is randomly distributed around zero. (D) The first three right SVs (colored dark blue, green, and red) also show structure, while the fourth SV (light blue) is a noiselike trace.

fluorescence traces were aligned to the time point at which half of the rising part of fluorescence was reached. Subsequently, each time-resolved fluorescence trace, which has m data points, is used as a column of a data matrix ($m \times n$ matrix **M**). Similarly, each fluorescence spectrum consisting of m data points is used as a column of another data matrix. The number of columns in this matrix, n, equals the number of samples with differing concentrations of denaturant. The size of the matrix containing time-resolved fluorescence data is 4087×24. The size of the matrix containing steady-state fluorescence spectra is 90×25. Singular-value decomposition (SVD) is the factorization of this matrix into three matrices: two of them composed of left and right singular vectors and one of them being a diagonal matrix with non-negative singular values ($\mathbf{M} = \mathbf{U\Sigma V^T}$).[10] $\mathbf{\Sigma}$ is the diagonal $m \times n$ matrix, and **U** and **V** are unitary matrices with dimensions of $m \times m$ and $n \times n$, respectively. The diagonal values of matrix $\mathbf{\Sigma}$ are the so-called singular values. The rank of matrix $\mathbf{\Sigma}$ determines the number of components. The columns of matrix **U** and matrix **V** are the left and right singular vectors, respectively, for the corresponding singular values and determine basis vector directions. Singular-value decomposition of the matrices of both experiments yielded a rank of matrix $\mathbf{\Sigma}$ equal to 3. The remaining singular values and associated singular vectors are attributed to noise. Therefore, three independent components are identified in the denaturation trajectory. These components arise from native and unfolded molecules, as well as folding intermediates.

Global Analysis. Prior to analysis of time-resolved data, fluorescence lifetimes and relative amplitudes corresponding to both native and unfolded apoflavodoxin molecules were estimated using samples containing 0 M GuHCl (i.e., all protein molecules are native) and 4 M GuHCl (i.e., all protein molecules are unfolded), respectively. These lifetimes and relative amplitudes were subsequently fixed during global analysis of the data

(three-exponential decay analysis was required for both folding states of the protein). In addition, we also used a three-exponential model to fit the fluorescence decay of the folding intermediate. Parameters that reflect the concentrations of the different folding species were allowed to change during the global fit procedure. In addition, the lifetimes and relative amplitudes associated with the folding intermediate were also allowed to change.

Global analysis of fluorescence anisotropy decay curves was performed as described in the following. The fluorescence decay of WFF apoflavodoxin in the absence of denaturant could be fitted to a triexponential decay function, whereas the fluorescence anisotropy decay of native WFF apoflavodoxin was monoexponential (i.e., having one correlation time and one amplitude). The fluorescence decay of WFF apoflavodoxin in the presence of 4 M denaturant (i.e., all protein molecules are unfolded) could be described by a triexponential decay function, whereas the fluorescence anisotropy decay of the unfolded protein required fitting with a biexponential function (i.e., two correlation times and two associated amplitudes). In the case of the folding intermediate coexisting with only the native state of WFF apoflavodoxin, experiments show that its fluorescence anisotropy decays monoexponentially. For all time-resolved fluorescence anisotropy traces of protein samples at denaturant concentrations ranging from 0 to 4 M GuHCl, the parameters that describe the biexponential anisotropy decay of unfolded protein molecules are fixed to the values obtained for unfolded WFF apoflavodoxin in 4 M GuHCl. The correlation times that describe the fluorescence anisotropy decay of native WFF apoflavodoxin and of its folding intermediate turn out to be identical at each concentration of denaturant used, and this value is allowed to change with an increase in denaturant concentration. The amplitudes of the monoexponential anisotropy decays
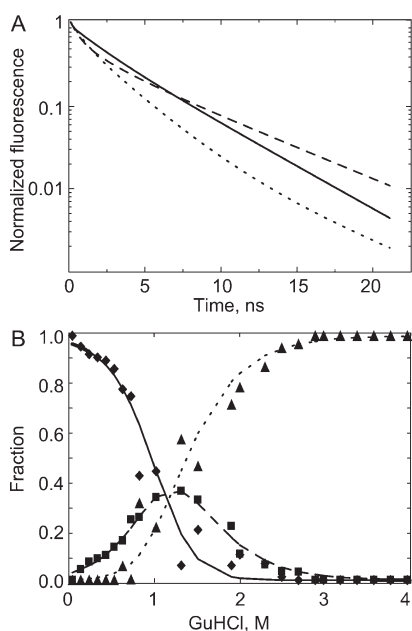
Figure 2. Analysis of time-resolved fluorescence data obtained from unfolding of WFF apoflavodoxin. (A) Fitted, normalized time-resolved fluorescence trace of WFF apoflavodoxin in 0 M GuHCl (native state, solid line) and the protein in 4 M GuHCl (unfolded state, dotted line). The normalized, triexponential fluorescence decay of the folding intermediate (dashed line) is derived from global analysis of all unfolding data. Table 1 collates fluorescence lifetimes and corresponding amplitudes of each folding species. (B) Relative concentrations of the different folding species as a function of denaturant concentration derived from global analysis of the data: (◆) native, (■) intermediate, and (▲) unfolded. Thermodynamic parameters derived from LAV analysis: $\Delta G_{IN}^{\circ} = -1.6$ kcal/mol, $\Delta G_{UI}^{\circ} = -2.0$ kcal/mol, $m_{IN} = 1.3$ kcal mol^{-1} M^{-1}, and $m_{UI} = 1.8$ kcal mol^{-1} M^{-1} (hence, $\Delta G_{UN}^{\circ} = -3.6$ kcal/mol, and $m_{UN} = 3.1$ kcal mol^{-1} M^{-1}).

belonging to the native state were linked to the amplitude of the monoexponential anisotropy decay of WFF apoflavodoxin without denaturant. The amplitude that describes the monoexponential anisotropy decay arising from the folding intermediate is set free during the global fitting procedure. Global analysis of both fluorescence decay and time-resolved fluorescence anisotropy was performed in an associative manner, allowing grouping of fluorescence lifetimes and relative amplitudes of each folding state with their corresponding anisotropy parameters.[14,15] Main output parameters of the fit of the denaturation trajectories are the rotational correlation times that describe slow tumbling of the different folding species and the fractional populations of each folding state involved.

Steady-state fluorescence spectra recorded for the protein at 0 and 4 M GuHCl are used as reference spectra that characterize native and unfolded molecules, respectively. The steady-state fluorescence spectrum of the folding intermediate was modeled as a skewed Gaussian and is described by three parameters: peak location, width, and skewness.[11,15] Spectra of the protein obtained at denaturant concentrations ranging from 0 to 4 M GuHCl were globally analyzed using a linear combination of reference spectra of native, unfolded, and intermediate folding species. The three parameters that describe the spectrum of the folding intermediate, as well as the relative concentrations of each folding species involved, were allowed to vary during global analysis. Full details of spectral fitting and global analysis are given in the Supporting Information.

Thermodynamic Analysis. As shown by Bollen et al.,[2] denaturant-induced equilibrium unfolding of apoflavodoxin is described by an N ↔ I ↔ U three-state model, in which N represents the native state, U represents unfolded molecules, and I is a folding intermediate. Consequently, the two corresponding equilibrium constants (i.e., K_{IN} and K_{UI}) and associated free energy differences (i.e., ΔG_{IN}° and ΔG_{UN}°) are

$$K_{IN} = \frac{[N]}{[I]} = \exp[-(\Delta G_{IN}^{\circ} + m_{IN}[D])/0.59]$$

$$K_{UI} = \frac{[I]}{[U]} = \exp[-(\Delta G_{UI}^{\circ} + m_{UI}[D])/0.59] \quad (1)$$

where m_{IN} and m_{UI} describe the denaturant dependence of ΔG_{IN}° and ΔG_{UI}°, respectively. The factor of 0.59 in this equation equals the gas constant R times temperature T (298 K) and is in units of kilocalories per mole. The fractional populations of each folding state (f_U, f_I, and f_N) follow from

$$f_U = \frac{1}{1 + K_{UI} + K_{IN}K_{UI}}$$

$$f_I = \frac{K_{UI}}{1 + K_{UI} + K_{IN}K_{UI}} \quad (2)$$

$$f_N = \frac{K_{IN}K_{UI}}{1 + K_{UI} + K_{IN}K_{UI}}$$

Global analysis yields the fractional populations of the folding species at a particular denaturant concentration, and these fractions were subsequently used to calculate ΔG_{IN}°, m_{IN}, ΔG_{UI}°, and m_{UI}. A least absolute value (LAV) approach was used during global analysis, because this approach is more robust against outliers than the least-squares method. During application of the LAV approach, the following function is minimized:

$$\min\left(\sum_i |f_{U*}^i - f_U^i| + |f_{I*}^i - f_I^i| + |f_{N*}^i - f_N^i|\right) \quad (3)$$

where f_U, f_I, and f_N are calculated with eq 2 and f_{U*}, f_{I*}, and f_{N*} are obtained using global analysis, with i being the summation index, which corresponds to the different concentrations of denaturant used. LAV analysis does not report standard errors.

■ RESULTS

Time-Resolved Fluorescence of Denaturant-Induced Unfolding of WFF Apoflavodoxin. Figure 1A presents the time-resolved fluorescence denaturation trajectory determined for WFF apoflavodoxin. Singular-value decomposition of the corresponding data matrix (Figure 1B) reveals the presence of three predominant singular values. The first three left singular vectors are shown in Figure 1C, and Figure 1D shows the first three right singular vectors. All other components have the signature of noise. Consequently, in the denaturation trajectory, three independent components can be ascribed to the presence of native and unfolded protein as well as a folding intermediate.

Fluorescence lifetimes and corresponding relative amplitudes of native and unfolded molecules are derived using time-resolved fluorescence data of apoflavodoxin in 0 and 4 M GuHCl, respectively. As described in Experimental Procedures, parameters that are allowed to float freely during the global fit procedure include fluorescence lifetime components and relative amplitudes associated with the folding intermediate as well as the relative concentrations of

each folding species involved. Normalized triexponential decay curves associated with the three folding species present are shown in Figure 2A, and Table 1 collates the corresponding amplitudes and fluorescence lifetime components. Figure 2B presents the relative concentrations of these species as a function of denaturant concentration and the fit of a three-state folding model to these data. This fit allows extraction of the free energy differences ΔG°_{IN} and ΔG°_{UI} and their dependencies on denaturant concentration, i.e., m_{IN} and m_{UI}, respectively (see detailed Experimental Procedures). ΔG°_{IN} is -1.6 kcal/mol, and ΔG°_{UI} is -2.0 kcal/mol (and m_{IN} and m_{UI} are 1.3 and 1.8 kcal mol^{-1} M^{-1}, respectively). Consequently, the difference in free energy between the unfolded and native protein, ΔG°_{UN}, is determined to be -3.6 kcal/mol.

Time-Resolved Fluorescence Anisotropy of Denaturant-Induced Unfolding of WFF Apoflavodoxin. In Figure 3, we present four of the time-resolved fluorescence anisotropy data sets of WFF apoflavodoxin obtained at increasing concentrations of GuHCl (selected data obtained at 0, 0.6, 2.0, and 4.0 M GuHCl). These data show that anisotropy decays slowly when WFF

apoflavodoxin is at low denaturant concentrations (i.e., 0 and 0.6 M GuHCl). In the case of the native protein, W74 is fixed within the interior of apoflavodoxin and thus exhibits overall rotational movements of the whole protein.[4] At 0.6 M GuHCl, 30% of all protein molecules are folding intermediates whereas the other molecules are native (Figure 2B), but anisotropy is still seen to decay slowly (Figure 3B). Thus, W74 must be equally well fixed within the molten globule-like folding intermediate of apoflavodoxin compared to that within native protein. At 2.0 M GuHCl, both the folding intermediate and the unfolded protein are present (Figure 2B), and now time-resolved anisotropy clearly consists of a rapidly decaying signal superimposed on a much more slowly decaying one (Figure 3C). Indeed, unfolded WFF apoflavodoxin, generated by increasing the GuHCl concentration to 4 M, is characterized by such rapidly decaying anisotropy. The following correlation times were obtained for unfolded protein at 4.0 M GuHCl: $\phi_1 = 0.35$ ns ($\beta_1 = 0.103$), and $\phi_2 = 2.49$ ns ($\beta_2 = 0.124$), yielding a β_1/β_2 value of 0.83 (see the legend of Figure 3D). These correlation times are typical for flexible polymers and reflect fast, almost unrestricted, segmental motions within the unfolded protein.

Figure 4 presents fit parameters of all individual anisotropy decay data, which are obtained at GuHCl concentrations ranging from 0 to 4 M (panel A shows amplitude ratios and panel B the observed correlation times). Up to 0.6 M GuHCl, a single, well-determined rotational correlation time of $10-12$ ns is observed. This correlation time is characteristic of tryptophan that is tightly incorporated into the protein and as a result exhibits overall rotational motions of apoflavodoxin. The corresponding β_2 values range from 0.22 to 0.24. At higher denaturant concentrations, the summation of β_1 and β_2 also lies in this range.

Table 1. Fluorescence Lifetime Components (τ) and Amplitudes (α) Derived from Three-Exponential Decay Analysis of the Denaturation Trajectory of WFF Apoflavodoxin[a]

species	α_1 (—)	τ_1 (ns)	α_2 (—)	τ_2 (ns)	α_3 (—)	τ_3 (ns)	$\langle\tau\rangle$ (ns)
native	0.10	0.14	0.29	1.95	0.61	4.30	3.20
folding intermediate	0.35	0.53	0.24	1.93	0.41	5.84	3.04
unfolded	0.29	0.73	0.65	2.54	0.06	6.06	2.23

[a] The sum of the amplitudes is normalized to 1 ($\sum_{i=1}^{3} \alpha_i = 1$). The first-order average fluorescence lifetime $\langle\tau\rangle$ equals $\sum_{i=1}^{3} \alpha_i\tau_i$.
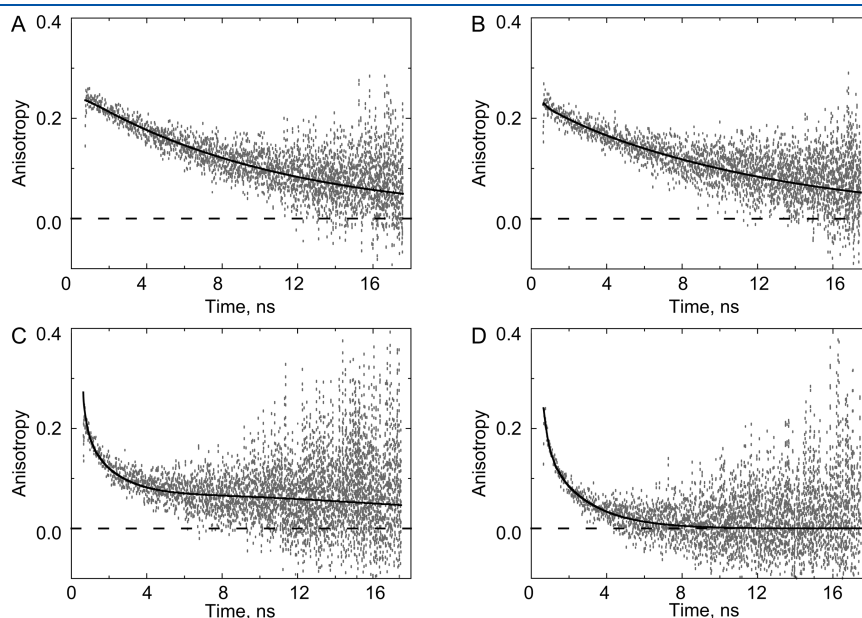

Figure 3. Experimental fluorescence anisotropy decay curves (gray dots) and associated fits (black lines) obtained for WFF apoflavodoxin at different stages of unfolding. (A) In 0 M GuHCl (the protein is native). The decay is fitted to $\beta_2 \exp(-t/\phi_2)$ with a β_2 of 0.24 and a ϕ_2 of 10.24 ns (67% confidence limits are $10.05-10.37$ ns) ($\chi^2 = 1.03$). (B) In 0.6 M GuHCl (native protein and a folding intermediate are present). The decay is fitted to $\beta_2 \exp(-t/\phi_2)$ with a β_2 of 0.22 and a ϕ_2 of 11.24 ns (67% confidence limits are $11.06-11.49$ ns) ($\chi^2 = 1.02$). (C) In 2.0 M GuHCl (folding intermediate and unfolded protein molecules are present). The decay is fitted to $\beta_1 \exp(-t/\phi_1) + \beta_2 \exp(-t/\phi_2)$ with a β_1 of 0.11 and a ϕ_1 of 0.67 ns (67% confidence limits are $0.58-0.82$ ns) and a β_2 of 0.12 and a ϕ_2 of 13.2 ns (67% confidence limits are $11.8-15.5$ ns) ($\chi^2 = 0.99$). (D) In 4.0 M GuHCl (only unfolded protein molecules are present). The decay is fitted to $\beta_1 \exp(-t/\phi_1) + \beta_2 \exp(-t/\phi_2)$ with a β_1 of 0.103 and a ϕ_1 of 0.35 ns (67% confidence limits are $0.21-0.39$ ns) and a β_2 of 0.124 and a ϕ_2 of 2.49 ns (67% confidence limits are $2.21-2.68$ ns) ($\chi^2 = 1.01$).
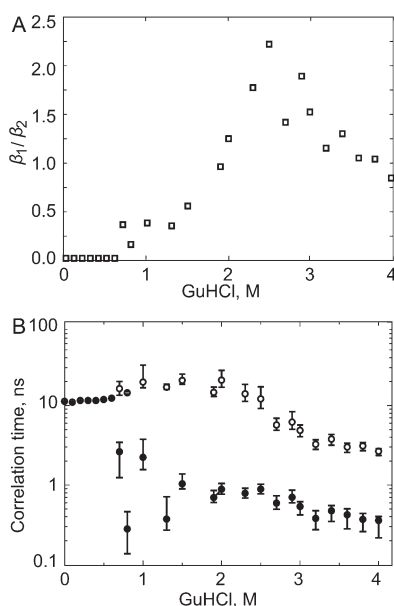
Figure 4. Parameters obtained upon fitting anisotropy decay data of WFF apoflavodoxin obtained at GuHCl concentrations ranging from 0 to 4 M. Up to 0.6 M GuHCl, a single-exponential decay $\beta_2 \exp(-t/\phi_2)$ suffices to describe the data. At higher denaturant concentrations, a biexponential decay function $\beta_1 \exp(-t/\phi_1) + \beta_2 \exp(-t/\phi_2)$ is required to describe the data. (A) Ratio of amplitudes β_1 and β_2. (B) Correlation times that describe slow (○) and fast (●) anisotropy decays with their confidence limits. The bars represent errors obtained with the exhaustive search approach.

Using the analysis strategy described in Experimental Procedures, we performed an associative global analysis of the denaturation trajectory as measured by time-resolved fluorescence anisotropy. Optimized parameters used in this analysis are, among others, the slow rotational correlation time that describes overall rotational motions of native protein and the folding intermediate and the denaturant-dependent population of the three folding states involved. Figure 5A presents the denaturant dependence of the slow correlation time and the predicted correlation times based on the increasing viscosity of aqueous solutions containing increasing denaturant concentrations.[16] In Figure 5B, the corresponding population of folding states is shown. The fit of a three-state folding model to the data of Figure 5B yields a $\Delta G^{\circ}_{\mathrm{IN}}$ of -2.1 kcal/mol and a $\Delta G^{\circ}_{\mathrm{UI}}$ of -1.7 kcal/mol (m_{IN} and m_{UI} values of 1.3 and 1.7 kcal mol^{-1} M^{-1}, respectively). Consequently, the difference in free energy between the unfolded and native protein, $\Delta G^{\circ}_{\mathrm{UN}}$, is determined to be -3.8 kcal/mol.

Steady-State Fluorescence Spectra of Denaturant-Induced Unfolding of WFF Apoflavodoxin. Figure 6A shows the denaturation trajectory of WFF apoflavodoxin as measured by steady-state fluorescence spectra. Singular-value decomposition of the corresponding data matrix suggests that the rank of this matrix is at least 3 (Figure 6B). The fourth left singular vector still shows structure (i.e., a peak at 333 nm), which we ascribe to the Raman background of water that is not properly subtracted from the data (Figure 6C). The fourth right singular vector has a noiselike appearance and does not have any structure (Figure 6D). The denaturation trajectory is globally analyzed using a linear combination of spectra resulting from native and unfolded protein, as well as from the folding intermediate. The
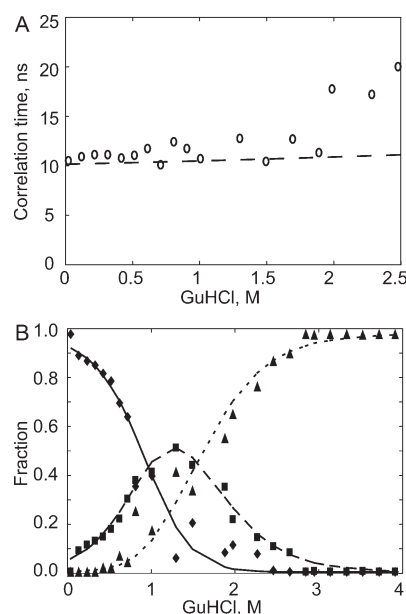

Figure 5. Analysis of time-resolved fluorescence anisotropy data obtained from WFF apoflavodoxin unfolding. (A) Denaturant dependence of the slow correlation time (nanoseconds) as derived from global analysis of the data. At >2.5 M GuHCl, this correlation time cannot be determined accurately and thus is not shown. The dashed curve is the expected increase in rotational correlation time based on the increase in viscosity with an increasing GuHCl concentration. The relative viscosity increase (η/η_0) as function of denaturant (D) concentration is obtained by the empirical relation published in ref 16: $\eta/\eta_0 = 1 + 0.005[D]^{1/2} + 0.018[D] + 0.01213[D]^{3/2}$. Because the rotational correlation time of the protein (ϕ) is proportional to the viscosity, the increase in correlation time with an increasing denaturant concentration can be obtained by multiplying ϕ by η/η_0. At 0 M GuHCl, we find experimentally $\phi = 10.2$ ns, and at 2.5 M GuHCl, we calculate $\phi = 11.3$ ns. (B) Relative concentrations of the different folding species as a function of denaturant concentration vs GuHCl concentration derived from global analysis: (◆) native, (■) intermediate, and (▲) unfolded. Thermodynamic parameters derived from LAV analysis are as follows: $\Delta G^{\circ}_{\mathrm{IN}} = -2.1$ kcal/mol, $\Delta G^{\circ}_{\mathrm{UI}} = -1.7$ kcal/mol, $m_{\mathrm{IN}} = 1.3$ kcal mol^{-1} M^{-1}, $m_{\mathrm{UI}} = 1.7$ kcal mol^{-1} M^{-1}, $\Delta G^{\circ}_{\mathrm{UN}} = -3.8$ kcal/mol, and $m_{\mathrm{UN}} = 3.0$ kcal mol^{-1} M^{-1}.

spectra corresponding with these folding species are shown in Figure 7A. The denaturant-dependent population of each folding state is presented in Figure 7B (full details of the analysis can be found in the Supporting Information). The fit of a three-state folding model to the data of Figure 7B yields a $\Delta G^{\circ}_{\mathrm{IN}}$ of -2.7 kcal/mol and a $\Delta G^{\circ}_{\mathrm{UI}}$ of -2.1 kcal/mol (Table 2; m_{IN} and m_{UI} values of 1.5 and 2.6 kcal mol^{-1} M^{-1}, respectively). Consequently, the difference in free energy between the unfolded and native protein, $\Delta G^{\circ}_{\mathrm{UN}}$, is determined to be -4.8 kcal/mol.

Steady-State Fluorescence Spectra of Double-Tryptophan-Containing Variants of Apoflavodoxin. We generated two double tryptophan variants of apoflavodoxin, namely, W74/W128/F167 (WWF) and W74/F128/W167 (WFW) apoflavodoxin. As described for WFF apoflavodoxin, steady-state fluorescence spectral denaturation trajectories of both apoflavodoxin variants were acquired and analyzed (see the Supporting Information for a detailed analysis). The denaturant-dependent population of each folding state observed is presented for WWF apoflavodoxin in Figure 8A and for WFW apoflavodoxin in
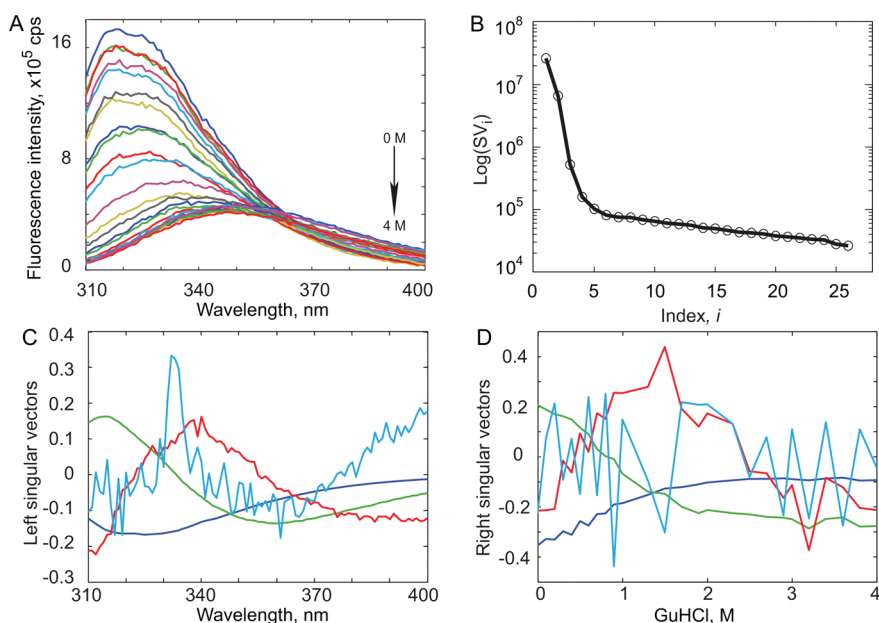
Figure 6. Analysis of steady-state fluorescence data obtained from denaturant-induced unfolding of WFF apoflavodoxin. (A) Denaturation trajectory of steady-state fluorescence spectra obtained at increasing concentrations of denaturant. (B) Singular-value decomposition of the corresponding data matrix shows the presence of at least three significant components (singular vectors, SVs). (C) The first four left SVs (colored dark blue, green, red, and light blue) show structure. (D) The first three right SVs (colored dark blue, green, and red) also show structure, while the fourth SV (light blue) is a noiselike trace.
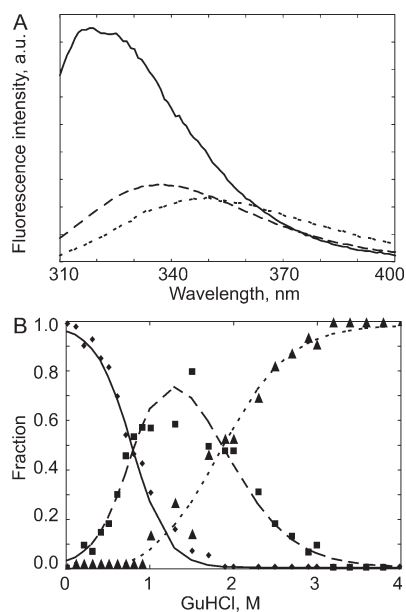

Figure 7. Analysis of steady-state fluorescence data obtained from WFF apoflavodoxin unfolding. (A) Steady-state fluorescence spectra of WFF apoflavodoxin in 0 M GuHCl (native protein, solid line) and 4 M GuHCl (unfolded protein, dotted line). The steady-state fluorescence spectrum of the folding intermediate (dashed line) is modeled as a skewed Gaussian and is derived from global analysis of all unfolding data. (B) Relative concentrations of the different folding species as a function of denaturant concentration derived from global analysis of the data: (◆) native, (■) intermediate, and (▲) unfolded. Thermodynamic parameters derived from LAV analysis of the data are listed in Table 2.

Figure 8B. The corresponding thermodynamic parameters are listed in Table 2.

■ DISCUSSION

In general, the fluorescence decay of single-tryptophan-containing proteins is complex,[17,18] because the side chain of tryptophan can exist in three predominant rotamers (for an overview, see refs 19 and 20 and references cited therein). As a result, one expects a three-exponential fluorescence decay curve with lifetimes characteristic of each rotameric state involved. The dissimilar fluorescence lifetimes reflect differences between rotamers in rates of excited-state electron transfer from the indole moiety to the amide group of the peptide bond.[19] The relative pre-exponential amplitudes of the three lifetime components agree with the relative populations of the corresponding rotameric states as revealed by ^{1}H NMR studies of rigid cyclic hexapeptides containing a single tryptophan.[19] The heterogeneity of the tryptophan environment has been corroborated by recent hybrid quantum mechanical and molecular mechanical simulations of both wavelengths and lifetimes for the six canonical rotamers of tryptophan in seven different hexapeptides in aqueous solution at room temperature.[20] The latter simulations reveal that rotamers having blue-shifted emission possess shorter average fluorescence lifetimes than those having red-shifted emission. Indeed, this study shows that the fluorescence decay of WFF apoflavodoxin is heterogeneous. To describe this decay, we require a minimal model that consists of three fluorescence lifetime components and corresponding amplitudes.

Because of the complexity of the fluorescence decay of tryptophan, interpretation of time-resolved fluorescence observations of denaturant-induced protein unfolding is not straightforward. Native WFF apoflavodoxin is shown here to give rise to the slowest average fluorescence lifetime, because the rotameric state with the largest lifetime (i.e., 4.3 ns) is predominantly populated, whereas the rotameric state that gives rise to the shortest fluorescence lifetime (i.e., 0.14 ns, which is due to considerable quenching) is hardly populated (Table 1). The tryptophan rotamer of the native protein that gives rise to the third observed

Table 2. Thermodynamic Parameters Obtained from GuHCl-Induced Equilibrium Unfolding of WFF Apoflavodoxin, WWF Apoflavodoxin, and WFW Apoflavodoxin[a]

	ΔG°_{UI} (kcal/mol)	m_{UI} (kcal mol^{-1} M^{-1})	ΔG°_{IN} (kcal/mol)	m_{IN} (kcal mol^{-1} M^{-1})	ΔG°_{UN} (kcal/mol)	m_{UN} (kcal mol^{-1} M^{-1})
WFF	−2.7	1.5	−2.1	2.6	−4.8	4.1
WWF	−2.9	1.5	−3.0	3.3	−5.9	4.8
WFW	−3.9	1.9	−2.9	3.0	−6.8	4.9

[a] A three-state model (N ⟷ I ⟷ U) is fitted to each individual denaturation trajectory, which is obtained by measuring steady-state fluorescence.
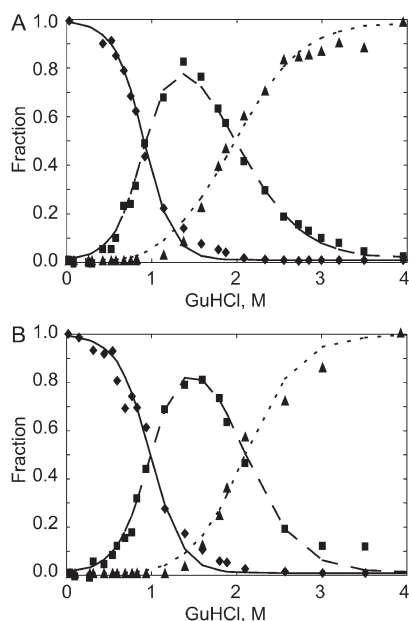

Figure 8. Relative concentrations of different folding species as a function of denaturant concentration derived from global analysis of denaturation trajectories of WWF (A) and WFW (B) apoflavodoxin: (◆) native, (■) intermediate, and (▲) unfolded. Denaturation trajectories are obtained by measuring steady-state fluorescence spectra. Thermodynamic parameters derived from LAV analysis of the data are listed in Table 2.

lifetime (i.e., 1.9 ns) is also present when the protein is present as a molten globule-like folding intermediate (Table 1) and is approximately equally populated for both folding species. In the case of the folding intermediate, the rotamer that gives rise to the 0.5 ns lifetime is more populated than the rotamer that causes the 5.8 ns lifetime. As a result, the average fluorescence lifetime of the folding intermediate is slightly shorter (i.e., 3.0 ns) than the lifetime that characterizes the native protein (i.e., 3.2 ns) (Table 1). In the case of the unfolded protein, rotameric states with short (i.e., 0.7 ns) and medium (i.e., 2.5 ns) lifetimes are predominantly populated, whereas the rotameric state with the longest lifetime (i.e., 6.0 ns) is hardly observed. Consequently, the average fluorescence lifetime of tryptophan in the unfolded protein [i.e., 2.2 ns (Table 1)] is the shortest of the values of all folding species observed.

Analysis of time-resolved anisotropy data of WFF apoflavodoxin unfolding reveals the remarkable observation that W74 is equally well fixed within both the native protein and the molten globule-like folding intermediate (Figures 3−5). Slight differences between the direct environments of W74 in the folding intermediate and native protein cause different rotameric populations of the indole in both folding species as fluorescence lifetime analysis reveals (Table 1). Unfolded protein is characterized

by a rapidly decaying fluorescence anisotropy component that is superimposed on a slower decaying component (Figure 3D). The correlation time that describes the slowly decaying component increases slightly with an increasing denaturant concentration, which can be explained in part by the increasing viscosity of the aqueous solution (Figure 5A). In addition, it was shown previously that the molten globule intermediate noncooperatively unfolds with an increasing denaturant concentration.[6] This partial unfolding causes an additional increase in the rotational correlation time of the protein.

Upon global analysis of the fluorescence data obtained from denaturant-induced unfolding of WFF apoflavodoxin, we determined the relative concentrations of the different folding species as a function of denaturant concentration (Figures 2B, 5B, and 7B). These data clearly show that a folding intermediate is formed during the unfolding of WFF apoflavodoxin. This intermediate folding state is maximally populated at ∼1.3 M GuHCl. Above ∼2 M denaturant, hardly any folding intermediate is present. The relative populations of the different folding states as estimated from time-resolved and steady-state fluorescence measurements differ somewhat, and as a result, slightly differing ΔG°_{UN} values are obtained (i.e., −3.6, −3.8, and −4.8 kcal/mol, respectively). This difference is probably caused by the measurement of (polarized) time-resolved fluorescence data at only one wavelength (i.e., 349 ± 3 nm), whereas steady-state fluorescence spectral data encompass information integrated over the whole wavelength region (310−400 nm) and time scale (i.e., first-order average fluorescence lifetime is proportional to relative fluorescence intensity at a particular wavelength). On basis of the available data, we estimate that the stability of WFF apoflavodoxin against global unfolding (i.e., ΔG°_{UN}) is −4.1 ± 0.6 kcal/mol.

The fluorescence emission spectrum of native WFF apoflavodoxin has a characteristic blue-shifted maximum [λ_{max} = 317 nm (Figure 6A)], also compared to those of the other apoflavodoxin variants used: λ_{max} = 322 nm for native WFW apoflavodoxin, λ_{max} = 330 nm for native WWF apoflavodoxin, and λ_{max} = 328 nm for native wild-type apoflavodoxin [4]. This blue-shifted maximum is indicative of a rigid, apolar environment around tryptophan.[21,22] On the basis of the list of experimental and calculated λ_{max} values of quite a number of single-tryptophan-containing proteins in ref 21, we judge that the environment of W74 in WFF apoflavodoxin falls in the same category as that of parvalbumin, which has one of the most blue-shifted emission maxima observed to date. Indeed, our time-resolved fluorescence anisotropy data (Figure 3A) show that W74 is fixed within the interior of the native protein and thus exhibits overall rotational movements of the whole protein.[4] The calculated steady-state fluorescence spectrum of the folding intermediate of WFF apoflavodoxin has a λ_{max} of 337 nm (Figure 7A). In contrast, the experimental fluorescence spectrum of the unfolded protein at 4 M GuHCl has a λ_{max} of 351 nm, which is characteristic for fully water-exposed tryptophan residues.

Importantly, thermodynamic analyses of the denaturation trajectories of the double-tryptophan-containing apoflavodoxin variants WWF (Figure 8A) and WFW (Figure 8B) show that these variants are significantly more stable against global unfolding than WFF apoflavodoxin [i.e., $-\Delta G^{\circ}_{UN}$ values of 5.9 and 6.8 kcal/mol, respectively (Table 2), vs 4.1 kcal/mol]. Hence, tryptophan residues contribute considerably to the thermodynamic stability of native apoflavodoxin. Indeed, native wild-type apoflavodoxin (i.e., WWW apoflavodoxin), which has three tryptophan residues, has a stability against global unfolding of 10.5 kcal/mol.[2] Altering just one tryptophan residue into phenylalanine already considerably lowers protein stability, whereas upon replacement of two tryptophan residues with phenylalanines, the protein stability is decreased even further.

■ ASSOCIATED CONTENT

S Supporting Information.   Details of the global analysis of steady-state fluorescence spectra with the help of a spectral model. This material is available free of charge via the Internet at http://pubs.acs.org.

■ AUTHOR INFORMATION

Corresponding Author
*E-mail: herbert.vanamerongen@wur.nl. Phone: +31 317 482634. Fax: +31 317 482725.

Present Addresses
∥Laboratoire d'Optique et Biosciences, CNRS UMR 7645, IN-SERM U696, Ecole Polytechnique, F-91128 Palaiseau, France. ⊥Department of Immunopathology, Sanquin Blood Supply Foundation, Plesmanlaan 125, 1066 CX Amsterdam, The Netherlands.

Author Contributions
S.P.L. and N.V.V. contributed equally to this work.

■ ABBREVIATIONS

ΔG°, free energy difference for folding; f, fractional population of a folding state; GuHCl, guanidine hydrochloride; K, equilibrium constant for folding; m, denaturant dependence of ΔG°; ϕ, correlation time from the fluorescence anisotropy decay; SV, singular vector; SVD, singular-value decomposition; τ, fluorescence lifetime; WFF, W74/F128/F167; WWF, W74/W128/F167; WFW, W74/F128/W167.

■ REFERENCES

(1) Eftink, M. R. (1994) The use of fluorescence methods to monitor unfolding transitions in proteins. *Biophys. J. 66*, 482–501.

(2) Bollen, Y. J. M., Sanchez, I. E., and van Mierlo, C. P. M. (2004) Formation of on- and off-pathway intermediates in the folding kinetics of *Azotobacter vinelandii* apoflavodoxin. *Biochemistry 43*, 10475–10489.

(3) Bollen, Y. J. M., Kamphuis, M. B., and van Mierlo, C. P. M. (2006) The folding energy landscape of apoflavodoxin is rugged: Hydrogen

exchange reveals nonproductive misfolded intermediates. *Proc. Natl. Acad. Sci. U.S.A. 103*, 4095–4100.

(4) Visser, N. V., Westphal, A. H., van Hoek, A., van Mierlo, C. P. M., Visser, A. J. W. G., and van Amerongen, H. (2008) Tryptophan-tryptophan energy migration as a tool to follow apoflavodoxin folding. *Biophys. J. 95*, 2462–2469.

(5) Engel, R., Westphal, A. H., Huberts, D. H., Nabuurs, S. M., Lindhoud, S., Visser, A. J. W. G., and van Mierlo, C. P. M. (2008) Macromolecular crowding compacts unfolded apoflavodoxin and causes severe aggregation of the off-pathway intermediate during apoflavodoxin folding. *J. Biol. Chem. 283*, 27383–27394.

(6) Nabuurs, S. M., Westphal, A. H., and van Mierlo, C. P. M. (2009) Noncooperative formation of the off-pathway molten globule during folding of the α-β parallel protein apoflavodoxin. *J. Am. Chem. Soc. 131*, 2739–2746.

(7) Alagaratnam, S., van Pouderoyen, G., Pijning, T., Dijkstra, B. W., Cavazzini, D., Rossi, G. L., Van Dongen, W. M., van Mierlo, C. P., van Berkel, W. J., and Canters, G. W. (2005) A crystallographic study of Cys69Ala flavodoxin II from *Azotobacter vinelandii*: Structural determinants of redox potential. *Protein Sci. 14*, 2284–2295.

(8) Steensma, E., and van Mierlo, C. P. (1998) Structural characterisation of apoflavodoxin shows that the location of the stable nucleus differs among proteins with a flavodoxin-like topology. *J. Mol. Biol. 282*, 653–666.

(9) Visser, N. V., Westphal, A. H., Nabuurs, S. M., van Hoek, A., van Mierlo, C. P., Visser, A. J., Broos, J., and van Amerongen, H. (2009) 5-Fluorotryptophan as dual probe for ground-state heterogeneity and excited-state dynamics in apoflavodoxin. *FEBS Lett. 583*, 2785–2788.

(10) Golub, G. H., and van Loan, C. F. (1996) *Matrix Computations*, 3rd ed., The Johns Hopkins University Press, Baltimore.

(11) van Stokkum, I. H. M., Larsen, D. S., and van Grondelle, R. (2004) Global and target analysis of time-resolved spectra. *Biochim. Biophys. Acta 1657*, 82–104.

(12) Beechem, J. M., Gratton, E., Ameloot, M., Knutson, J. R., and Brand, L. (1991) The global analysis of fluorescence intensity and anisotropy decay data: Second generation theory and programs. In *Topics in Fluorescence Spectroscopy* (Lakowicz, J. R., Ed.) Vol. 2, pp 241–305, Plenum Press, New York.

(13) Beechem, J. M. (1992) Global analysis of biochemical and biophysical data. *Methods Enzymol. 210*, 37–54.

(14) Digris, A. V., Skakoun, V. V., Novikov, E. G., van Hoek, A., Claiborne, A., and Visser, A. J. W. G. (1999) Thermal stability of a flavoprotein assessed from associative analysis of polarized time-resolved fluorescence spectroscopy. *Eur. Biophys. J. 28*, 526–531.

(15) van Stokkum, I. H. M., Linsdell, H., Hadden, J. M., Haris, P. I., Chapman, D., and Bloemendal, M. (1995) Temperature-induced changes in protein structures studied by Fourier-transform infrared-spectroscopy and global analysis. *Biochemistry 34*, 10508–10518.

(16) Kawahara, K., and Tanford, C. (1966) Viscosity and density of aqueous solutions of urea and guanidine hydrochloride. *J. Biol. Chem. 241*, 3228–3232.

(17) Larsen, O. F. A., van Stokkum, I. H. M., Pandit, A., van Grondelle, R., and van Amerongen, H. (2003) Ultrafast polarized fluorescence measurements on tryptophan and a tryptophan-containing peptide. *J. Phys. Chem. B 107*, 3080–3085.

(18) Pandit, A., Larsen, O. F. A., van Stokkum, I. H. M., van Grondelle, R., Kraayenhof, R., and van Amerongen, H. (2003) Ultrafast polarized fluorescence measurements on monomeric and self-associated melittin. *J. Phys. Chem. B 107*, 3086–3090.

(19) Adams, P. D., Chen, Y., Ma, K., Zagorski, M. G., Sonnichsen, F. D., McLaughlin, M. L., and Barkley, M. D. (2002) Intramolecular quenching of tryptophan fluorescence by the peptide bond in cyclic hexapeptides. *J. Am. Chem. Soc. 124*, 9278–9286.

(20) Pan, C.-P., Muiño, P. L., Barkley, M. D., and Callis, P. R. (2011) Correlation of tryptophan fluorescence spectral shifts and lifetimes arising directly from heterogeneous environment. *J. Phys. Chem. B 115*, 3245–3253.

(21) Vivian, J. T., and Callis, P. R. (2001) Mechanisms of tryptophan fluorescence shifts in proteins. *Biophys. J. 80*, 2093–2109.

(22) Broos, J., Tveen-Jensen, K., de Waal, E., Hesp, B. H., Jackson, J. B., Canters, G. W., and Callis, P. R. (2007) The emitting state of tryptophan in proteins with highly blue-shifted fluorescence. *Angew. Chem., Int. Ed. 46*, 5137–5139.